CO_2 laser absorption measurements of temperature and density in the shock-induced Richtmyer-Meshkov mixing zone

J. Fortes, A. Ramdani, and L. Houas
Université de Provence, Institut Universitaire des Systèmes Thermiques Industriels, Centre National de la Recherche Scientifique, URA 1168, Departement MHEQ, Faculté Saint Jérôme, 13397 Marseille Cedex 20, France
(Received 28 March 1994)

The aim of this paper is to discuss the interest of using spectroscopic diagnostic methods to study shock-induced Richtmyer-Meshkov mixing as a complement to other experimental techniques, numerical simulations, and theoretical studies. Using a CO_2 laser absorption technique, the average temperatures and densities are experimentally determined through a high velocity gaseous mixing zone. This mixing is originated from a shock-induced acceleration of a plane interface, materialized by a thin plastic membrane, that initially separates two gases of different densities. Two gas combinations have been tested: CO_2-Ar and CO_2-He. Temperature and density are determined within the shock accelerated mixing zone from infrared absorption measurements of two characteristic vibrational-rotational lines of the CO_2 bending mode, using a CO_2 continuous wave laser as a diagnostic probe. The absorption coefficient is a function of the temperature and density of the CO_2 for a known linewidth profile. Thus, temperature and density profiles within the mixing region are calculated from two measurements. For this, a CO_2 absorption coefficient model, assuming the Voigt linewidth profile in the mixing region and taking into account the contribution of the hot bands, has been developed. It is shown that the technique is well applicable to this type of study, and that there is a strong correlation between the Atwood number and the shape of the mixing zone.

PACS number(s): 52.35.Tc, 52.40.Nk

I. INTRODUCTION

A. Richtmyer-Meshkov instability

In the context of inertial confinement fusion (ICF) an experimental work is undertaken to analyze the impulsive Rayleigh-Taylor instability. This instability is one of the causes of the generation and development of a turbulent mixing zone, between the shell material and the thermonuclear combustible of an ICF pellet, which contributes to reducing the efficiency of the nuclear reaction by early breakup of the shell and cooling of the combustible.

The absorption method presented in this work has been developed for studying, in the simpler shock tube environment, the evolution of the mixing zone created by the interaction of a high Mach number shock wave and a gaseous interface initially at rest. When a shock wave accelerates the interface, this one is subjected to the impulsive Rayleigh-Taylor [1,2] instability, also called the Richtmyer-Meshkov [3,4] instability. If the membrane is initially planar, which is the case for the experiments presented in this paper, only the random small spatial scales created by the membrane breakup are excited and the turbulent mixing occurs soon.

In most of the experimental studies on the development of mixing regions due to Rayleigh-Taylor or Richtmyer-Meshkov instabilities, results are based on the determination of the mixing zone thickness, because it allows one to determine the turbulent energy developing within the mixing region. But, up to now, few measurement techniques have been developed to determine quantitatively the thermodynamic parameters in the mixing zone, such as temperature or density. Recently, Mikaelian [5] gave calculated turbulent energy profiles within shock accelerated interfaces, but, for this study, he supposes a linear density profile in the turbulent mixing region, and he suggests that more experimental results are needed.

Because of its spectroscopic properties in the infrared band, CO_2 has been used as one of the two constituting gases of the mixing zone. The other constituent is argon or helium because each presents no infrared emission or absorption in the domain of our experiments. Furthermore, as their densities are, respectively, very different and close to that of CO_2, one can study the influence of the gas density gradients on the mixing.

B. Laser absorption principle of measurements

The laser absorption technique has been described by Wang [6] to measure temperature and concentration species through a radiating flow. He used an absorption coefficient corresponding to two or more monochromatic lines according to one or more absorbing species present in the burning media. He also shows that it is possible to determine temperature and concentration distributions in nonhomogeneous media with absorption measurements in different directions. Hanson and Falcone [7] use two vibrational-rotational lines of CO, centered on 4.7 μm, to measure the temperature of a medium resulting from the combustion of a propane and air mixture at atmospheric pressure. Cheng and Bien [8] study the case of an axisymmetric medium composed of methane and burning carbon. They measure the absorption of two rotational-

vibrational lines of CO at different parallel positions. But as the medium studied was strongly nonhomogeneous, they were obliged to realize an Abel inversion to obtain the temperature distribution of the mixing along the radius of the shock tube.

The same technique has been used by Rea and Hanson [9] to determine temperature in the postflame region corresponding to a hydrocarbon-air combustion. The authors give temperature profiles analogous to those that we have obtained within the mixing zone. We have adapted this technique for our study. However, the mixing region in our case is composed of CO_2-He or CO_2-Ar, which renders the problem easier because there is only one absorbing species. We have neglected the effects of the boundary layer, which is colder than the main flow, on the crossing of the laser beam. Furthermore, we have shown in Ref. [10] that when the initial interface is plane, the deformation of the mixing zone front is the lowest. Thus, the temperature and density obtained by integration over the laser beam trajectory are average values.

In this paper we present results obtained with a CO_2 laser absorption technique which has already been presented in Ref. [11] in its first approach. Now, a more rigorous absorption coefficient model is developed.

II. EXPERIMENTAL SETUP AND INITIAL CONDITIONS

A. Experimental setup

Figure 1 represents the experimental setup for the absorption measurements. Experiments are carried out in a double diaphragm shock tube, of 8.5×8.5 cm^2 cross section and length about 9 m. The test section is about 1.5 m long downstream from the second diaphragm. The gases, carbon dioxide upstream and helium or argon downstream, are initially separated by a thin plastic film (1.5 μm) which constitutes the second diaphragm. The driver gas is hydrogen. Before introducing the test gases, a vacuum of about 10^{-3} Torr is obtained on both sides of the thin membrane, using a rotary pump followed by a diffusion pump. During the phases of pumping and introducing gases, the maximum amplitude of the initial deformation of the membrane is less than 1 mm. These two phases are the most delicate operations in the preparation of the experiments. Wall heat transfer gauges are used to determine the velocity of the shock wave, with an error on the Mach number less than 3%, while the velocity of the mixing zone is obtained, with the same accuracy, from two simultaneous CO_2 emission measurements at different abscissas, taken during the same absorption run. The trigger signal is given by the shock wave passage in front of one of the wall gauges, and then suitably delayed.

We use a CO_2 continuous wave laser beam, Model 81-5500-T, from California Laser, 1 mm diameter, 8.8 mrad aperture angle and 2 mm-diam spot at 40 cm distance, 7 W maximum power, 10.4 μm centered wavelength, and 425 ± 25 MHz width under standard operating conditions. Out of these standard operating conditions, which require 1–2 h continuous running in a stabilized temperature room before performing the experiments, one can witness an important broadening rate, up to 200 MHz/°C, and, as a consequence, an important decrease of the laser power for a given wavelength. This laser operates on the rotational-vibrational transition 00°1-10°0 of the CO_2 molecule and for different characteristic lines of this transition. Therefore, for each experiment, the laser emission line is controlled with both a powermeter and a spectrum analyzer.

Infrared absorption of CO_2 is collected with a liquid nitrogen cooled photovoltaic $Cd_xH_{1-x}Te$ detector. The response time of the detector is less than 1 μs and its passband is centered at 10.4 μm. As indicated in Fig. 1, the initial laser beam intensity is strongly reduced by the ZnSe and Ge attenuators so that its power is less than 10 mW when it arrives on the sensitive infrared detector cell.

B. Initial conditions

Measurements are essentially based on infrared absorption of shock heated CO_2. The infrared technique requires strong shocks—Mach 4 in CO_2, 3.7 and 2 in Ar and He, respectively—and therefore the velocities behind the shock, 700 m/s for the CO_2-Ar interface and 1060 m/s for the CO_2-He one, are into the compressible range. The initial pressure of the gases on both sides of the plastic membrane is the same, about 2000 Pa, in all the experiments, in order to avoid any large scale initial bulge [10]. The use of two gas pairs, CO_2-He and CO_2-Ar, allows to analyze the influence of the Atwood number ($|A_t|_{CO_2\text{-He}}\approx0.80$ and $|A_t|_{CO_2\text{-Ar}}\approx0.26$) on the subsequent turbulent mixing. The Atwood number is defined by

$$A_t=\frac{\rho_{(\text{Ar or He})}-\rho_{CO_2}}{\rho_{(\text{Ar or He})}+\rho_{CO_2}},$$

where ρ_i is the density of the gas i just after the shock passage. Average temperature and CO_2 density profiles have been obtained at the abscissa of 940 mm from the initial position of the interface, which corresponds to a time of 1340 μs for the CO_2-Ar mixing zone and 886 μs for the CO_2-He mixing zone.

III. ANALYTICAL MODEL OF THE CO_2 ABSORPTION COEFFICIENT IN THE MIXING ZONE

The knowledge of the absorption coefficient of an optical active medium allows us to know the thermodynamic state of this medium. In the context of our work, we have to obtain some information on the thermodynamic state of a turbulent gaseous mixing zone (CO_2-He or CO_2-Ar), moving at high velocities in a shock tube. For this, we need to know the absorption coefficient of the CO_2 molecule, in the gaseous mixings CO_2-He or CO_2-Ar for the transition Σ (00°1-10°0) when these media are traversed by a low power continuous CO_2 laser beam [12,13].

We use the semiclassical theory of wave-matter interaction. The absorption coefficient is the result of the contributions of the laser induced absorption and emission as well as the spontaneous emission. We have taken into account the spectral width of the laser line and the spectral width of the CO_2 absorption line in the test section. This CO_2 absorption line is a function of the Doppler width due to the thermal molecular motion, the collisional width dependent on the gas pressure and temperature in the considered medium, and its composition: that is, a CO_2 Voigt profile [14]. We also have taken into account the hot bands of the Σ (00°1-100°) transition which can give a non-negligible contribution to the absorption coefficient [15]. Thus, we have realized a theoretical model of the absorption coefficient of the CO_2 molecule in gaseous mixing media, CO_2-Ar or CO_2-He, which takes into account all the contributions previously described.

A. The absorption coefficient

Let us consider an absorbing medium with an elementary thickness dl, crossed by a low intensity radiation I_0

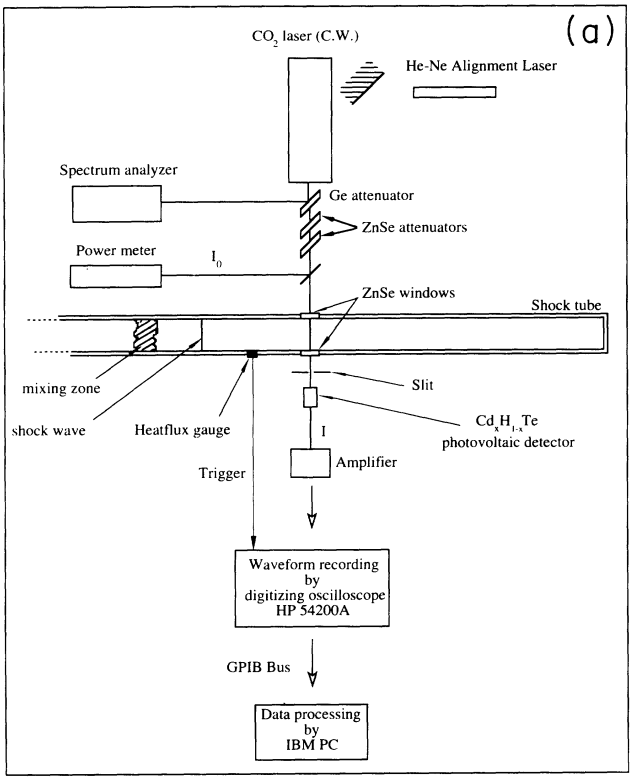

FIG. 1. (a) Sketch of the experimental set-up; (b) typical absorption signal record.

Absorption signal of CO_2 -Ar mixing;Mach number 4

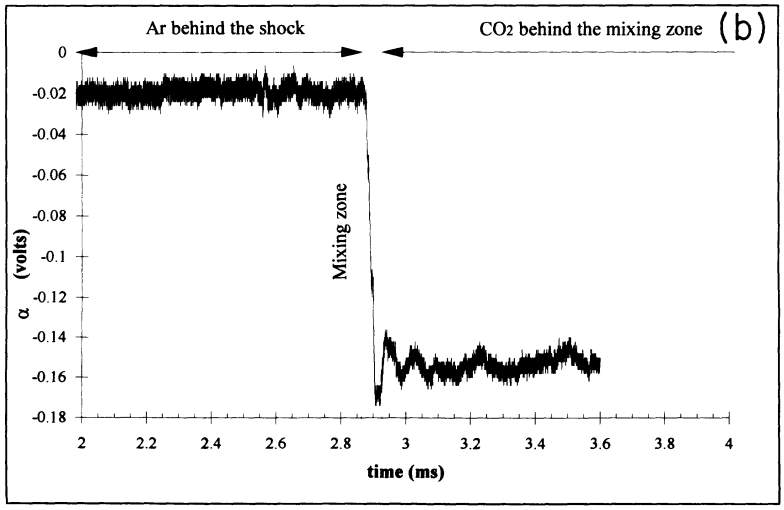

with a frequency ν. The intensity of this radiation changes of a quantity dI which is proportional to the incident intensity as predicted by the Bourguer-Lambert [16] law:

$$dI=-\alpha I\,dl\ , \tag{1}$$

where α is a coefficient of proportionality called the absorption coefficient and I the intensity after absorption. The integration of Eq. (1) along the distance L gives the expression of the absorption coefficient α:

$$\alpha=\frac{1}{L}\ln\left[\frac{I_0}{I}\right]\ . \tag{2}$$

Let us now consider a system of particles submitted to a radiation I_0 with the frequency ν. Let N_l be the number of molecules in the fundamental quantic state and N_u the number of molecules in the quantic excited state. Then, $\rho_{\nu lu}$, the density of the energy of the incident radiation, is [16,17]:

$$\rho_{\nu lu}=\frac{8\pi h\nu_{lu}^3}{c^3}\frac{1}{e^{h\nu_{lu}/KT}-1}\ . \tag{3}$$

Assuming thermodynamical equilibrium, there is equality between induced absorption, spontaneous emission, and isotropic induced emission:

$$N_uB_{u-l}\rho_{\nu lu}+N_u\,A_{u-l}=N_lB_{l-u}\rho_{\nu lu}\ . \tag{4}$$

With the classical hypothesis of a Boltzmann distribution function for the population of the transition levels [16]:

$$\frac{N_l}{N_u}=g_le^{-h\nu_{lu}/KT} \tag{5}$$

and

$$g_lB_{l-u}=g_uB_{u-l}\ , \tag{6}$$

we obtain

$$A_{u-l}=\frac{8\pi h\nu_{lu}^3}{c^3}B_{u-l}\ , \tag{7}$$

where N and g correspond, respectively, to the population and the statistic weight of each considered level; A and B are the Einstein coefficients; l and u the lower and upper level indices, respectively; h and K are the Planck and Boltzmann constants, respectively; and c the velocity of light. If we suppose that the intensity variation dI of the incident radiation is due to induced emission and absorption, then we obtain

$$dI=\frac{h\nu}{c}(N_uB_{u-l}-N_lB_{l-u})I\,dl\ , \tag{8}$$

and combining relations (2), (6), (7), and (8),

$$\alpha=\frac{h\nu}{c}g_lB_{l-u}\left[\frac{N_l}{g_l}-\frac{N_u}{g_u}\right]\ . \tag{9}$$

In the semiclassical theory framework of the radiation-matter interaction, B_{u-l} is given by [16–19]

$$B_{u-l}=\frac{8\pi^3}{3h^2}|R_{12}|^2|R_{jj'}|^2Hf(\nu-\nu_0)\ , \tag{10}$$

where R_{12} is the matrix element term of the dipolar electrical moment depending on the change of the vibrational level, $R_{jj'}$ the matrix element term of the dipolar electrical moment depending on the change of the rotational level given by [18,19]

$$|R_{jj'}|=\frac{S_{j'l'}}{g_j}\quad\text{and}\quad S_{j'l'}=\frac{m^2-l^2}{m}\ , \tag{11}$$

and $H=1-C_1m-C_2m^2$ is the term which takes into account the rotational-vibrational interaction (~ 1 for CO_2), $m=j$ or $j+1$, $C_1\sim 10^{-3}$ and $C_2\sim(6\pm1)\times10^{-5}$ are two constants, and $f(\nu-\nu_0)$ the spectral profile of the incident radiation absorption line.

Thus, Eq. (9) becomes

$$\alpha=\frac{8\pi^3\nu}{3hc}g_l|R_{JJ'}|^2|R_{12}|^2Hf(\nu-\nu_0)\left[\frac{N_l}{g_l}-\frac{N_u}{g_u}\right]\ . \tag{12}$$

The spectral profile $f(\nu-\nu_0)$ of the incident radiation is a Voigt profile. In the case of the CO_2-Ar or CO_2-He combination of gaseous mixings, it is given by [12,18]

$$f_{\text{Voigt}}(\nu)=\frac{a}{\pi\Delta\nu_D}\left[\frac{\ln 2}{\pi}\right]^{1/2}\int_{-\infty}^{+\infty}\frac{e^{-y^2}}{a^2+(x-y)^2}dy\ , \tag{13}$$

with

$$x=\sqrt{\ln 2}\frac{(\nu-\nu_0)}{\Delta\nu_D}\ ,\quad a=\ln 2\frac{\Delta\nu_c}{\Delta\nu_D}\ ,$$

and where $\Delta\nu_c$ is the collisional profile depending on the pressure and temperature of the gaseous mixing, $\Delta\nu_D$ is the Doppler profile which is characteristic of the thermal motion in the medium, and $\Delta\nu_c$ and $\Delta\nu_D$ are given by [18,19]

$$\Delta\nu_c=CP\gamma_{CO_2\text{-}CO_2}^{(j)}\left[\psi_{CO_2}\left[\frac{300}{T}\right]^{n_{CO_2\text{-}CO_2}}+\sum_i\psi_X\left[\frac{300}{T}\right]^{n_{CO_2\text{-}X}}\times\left[\frac{\gamma_{CO_2\text{-}X}^{(j)}}{\gamma_{CO_2-CO_2}^{(j)}}\right]\right]\ , \tag{14}$$

with

$$C=1.65\times10^{-4}\ \text{m}^2\text{K}^{1/2}\,\text{kg}^{-1/2}$$

and

$$\Delta\nu_D=2\nu_0\left[\frac{2\ln(2)KT}{Mc^2}\right]^{1/2}\ , \tag{15}$$

where Ψ_{CO_2} is the mass concentration of CO_2 in the mixing CO_2-X (X=Ar, He), Ψ_X is the mass concentration of

argon or helium in the mixing CO_2-X, and

$$M=\frac{M_{CO_2}M_x}{M_{CO_2}+M_x} .$$

B. General expression of the CO_2 absorption coefficient taking into account the hot bands

For a given line of the CO_2 infrared spectrum, one can find adjacent lines in near resonance with it which contribute to the absorption of the CO_2 in this band in a non-negligible quantity ($\leq 40\%$). These bands are called "hot bands." Therefore, we have determined the bands contributing to the total absorption of the CO_2 for the transition Σ (00°1-100°) and calculated the percentage of the population of the low level transitions centered on a frequency near 961 cm^{-1} (10.4 μm). Transitions whose low levels have a population that may be considered as low are neglected, and the others are what we call hot bands. We have considered all the hot bands in resonance with the absorption line likely to contribute to the absorption.

Figure 2(a) schematizes the configurations that we have used in the present work, which are a laser beam of frequency ν_0 and width $\Delta\nu_0$ and the two hot bands adjacent to the principal absorption band the spectral range of which is about of the order of the absorption line. Thus, the total absorption coefficient represents the sum of the contribution of the principal band and the contribution of the hot bands:

$$\alpha=\alpha_0+\sum_{i=1}^{n}\alpha_i , \tag{16}$$

where α_0 is the absorption coefficient of the principal band and α_i the absorption coefficient of the ith hot band.

Figure 2(b) represents the profiles of the principal CO_2 band and the laser. Within the hypothesis of a Voigt profile [relation (13)] the resonant absorption coefficient of the centered line is

$$\alpha_0=\frac{1}{\Delta\nu_0}\int_{\nu_0-\Delta\nu_0/2}^{\nu_0+\Delta\nu_0/2}\alpha_0^0(\nu)f_0(\nu)d\nu , \tag{17}$$

where α_0^0 is given by relation [12].

Now, considering $\Delta\nu_0/\nu_0$ as a small quantity, and [18,19]

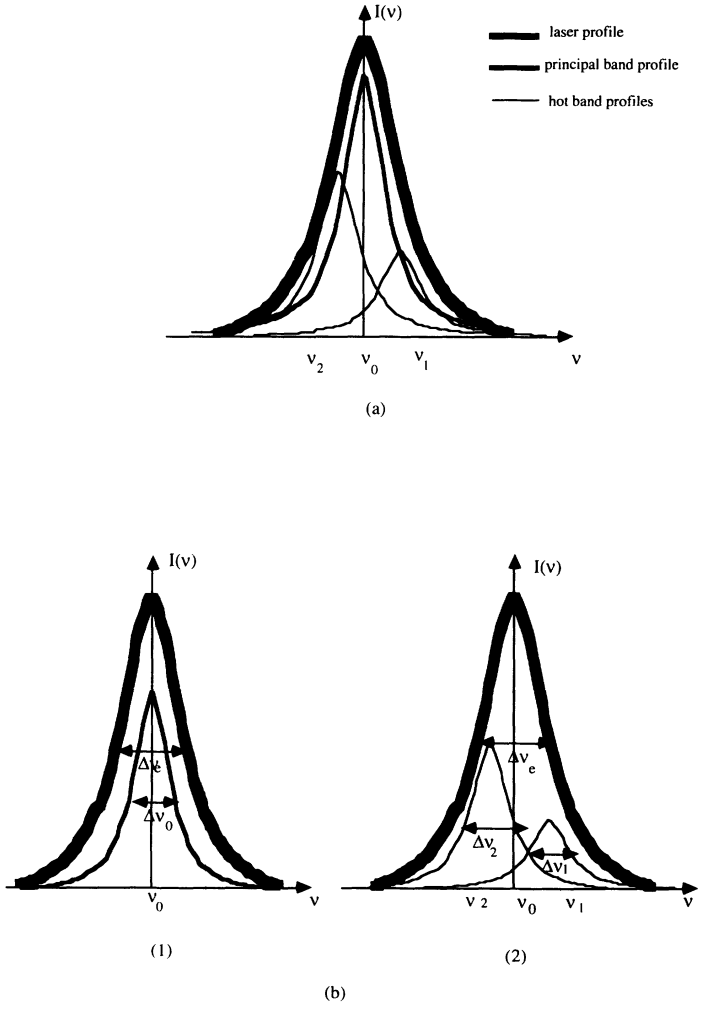

FIG. 2. (a) Spectral profile of 10.4-μm CO_2 laser and CO_2 absorption line and its hot bands; (b) case (1): spectral profile of 10.4 μm CO_2 laser and CO_2 absorption line without hot bands, and case (2): spectral profile of 10.4 μm CO_2 laser and CO_2 absorption line with its hot bands.

$$\frac{a}{\pi}\int_{-\infty}^{+\infty}\frac{e^{-y^2}}{a^2+(y)^2}dy=\exp(a^2)[1-\mathrm{erf}(a)]\ , \tag{18}$$

with

$$\mathrm{erf}(x)=\frac{2}{\sqrt{\pi}}\int_0^x e^{-z^2}dz\ ,$$

relation (17) becomes:

$$\alpha_0(\nu)=\alpha_0^0(\nu)\left[\frac{\ln 2}{\pi}\right]^{1/2}\exp(a^2)[1-\mathrm{erf}(a)]\ . \tag{19}$$

The CO_2 hot band profiles and their positions relative to the center of the laser line are schematized in Fig. 2(b). As previously said, when taking into account the nonadjustment of the laser line and the ith hot band, we define a new profile:

$$g_i(\nu)=f_{\mathrm{Voigt},i}(\nu)\ f_L(\nu_0+k_i+\nu_i i)\ , \tag{20}$$

where $f_{\mathrm{Voigt},i}(\nu)$ is the Voigt profile for the hot band i and $f_L(\nu_0+k_i+\nu_i)$ is the value of the laser line profile, assumed to be Lorentzian, on the point $\nu=\nu_0+k_i+\nu$, ν_0 being the laser line frequency, ν_i the ith hot band frequency, k_i the distance between them, and

$$f_L(\nu)=\frac{1}{\pi}\frac{1}{1+4\left\{\dfrac{k_i}{\Delta\nu_c}+\dfrac{x_i\Delta\nu_D}{\sqrt{\ln 2}\Delta\nu_c}\right\}^2}\ . \tag{21}$$

Then, the absorption coefficient of the ith hot band is

$$\alpha_i=\frac{1}{\Delta\nu_i}\int_{\nu_i-\frac{\Delta\nu_i}{2}}^{\nu_i+\frac{\Delta\nu_i}{2}}\alpha_i^0(\nu)g_i(\nu)d\nu\ , \tag{22}$$

where α_i^0 is defined by relation (12) and $f_i(\nu)$ by relation (13).

With the hypothesis of a Voit profile, the absorption coefficient for the ith hot band becomes

$$\alpha_i=\frac{2\Delta\nu_D\alpha_i^0(\nu)a}{\pi^{3/2}\Delta\nu_i}\int_{\nu_i-\nu_i/2}^{\nu_i+\nu_i/2}\int_{-\infty}^{+\infty}\left\{\frac{e^{-y^2}}{a^2+(x_i-y)^2}\right\}\frac{1}{1+4\left\{\dfrac{k_i}{\Delta\nu_c}+\dfrac{x_i\Delta\nu_D}{\sqrt{\ln 2}\Delta\nu_c}\right\}^2}\ , \tag{23}$$

with

$$x_i=\frac{(\nu-\nu_i)}{\nu_D}\sqrt{\ln 2}\ ,\quad \Delta x_i=\frac{\Delta\nu}{\nu_D}\sqrt{\ln 2}\ .$$

If we suppose that the normalized width is smaller than 1, we can develop α_i around zero:

$$\alpha_i(\Delta x_i)=\alpha_i(0)+(\Delta x_i)\alpha_i(0)+o(\Delta x_i^n)\ , \tag{24}$$

and considering $\Gamma'(x_i)$,

$$\Gamma'(x_i)=\frac{1}{1+4\left\{\dfrac{k_i}{\Delta\nu_c}+\dfrac{x_i\Delta\nu_D}{\sqrt{\ln 2}\Delta\nu_c}\right\}^2}\ , \tag{25}$$

with x_i small, the development of $\Gamma'(x_i)$ near zero gives

$$\Gamma'(x_i)=\frac{1}{1+4\left\{\dfrac{k_i}{\Delta\nu_c}\right\}^2}-8\left\{\frac{(k_i-\nu_i)\Delta\nu_c^2}{\Delta\nu_c^2\sqrt{\ln 2}}\right\}\times\frac{1}{\left[1+4\left\{\dfrac{k_i}{\Delta\nu_c}\right\}^2\right]^2}\ , \tag{26}$$

then the corresponding absorption coefficient α_i can be written

$$\alpha_i(\nu)=\alpha_i^0(\nu)\frac{\Delta\nu_i}{\Delta\nu_D}\frac{1}{\left[1+4\left\{\dfrac{k_i}{\Delta\nu_c}\right\}^2\right]}\times\left[\frac{\ln 2}{\pi}\right]^{1/2}\exp(a^2)[1-\mathrm{erf}(a)]\ . \tag{27}$$

Finally, the general expression of the absorption coefficient is

$$\alpha_\omega(\rho,T)=\frac{8\pi_j^3\nu_0}{3KT}\left[\frac{\ln 2}{\pi}\right]^{1/2}|R_{12}|^2|R_{jj'}|^2\rho_{\mathrm{CO}_2}Q_v^{-1}\times\exp(a^2)\left\{\frac{\sqrt{\pi/2}}{a+\{[(\pi-2)a/2]^q+p^2/4\}^{1/q}}\right\}\times\sum_i\alpha(j_i,T)\ , \tag{28}$$

with

$$\alpha(j_i,T)=\left\{b_1e^{-[b_1j_i(j_i+1)hc]/KT}-b_2e^{[-b_2(j_i+j')(j_i+j'+1)hc]/KT}\right\}\left\{1+\frac{1}{\left[1+4\left\{\dfrac{k_i}{\Delta\nu_c}\right\}^2\right]}\frac{|R_{i,12}'^2|}{|R_{12}^2|}\right\}\ ,$$

where j_i is the rotational number of the ith hot band, $j'=0$ for an R line, $j'=-1$ for a P line, $R'_{i,12}$ is the intensity of the ith hot band of the considered transition, $p \approx 1.902$, and, finally, $i=0$ corresponds to the principal band for which $k_i=0$.

IV. TEMPERATURE AND DENSITY CALCULATION

If we suppose that the rotational-vibrational lines of CO_2 transitional band $0°01-1°00$ are completely separated and if the gap between two nearby lines is larger than 27 GHz and the spectral width of each absorption line smaller than 2 GHz (for a pressure range less than 5 atm), one can assume that the absorption coefficient for a given line is only a function of its spectral and hot band properties. Furthermore, as the pressure ratio between the CO_2 in the shock tube and the CO_2 in the laser cavity is less than 10, we can neglect [14] the shift between the absorption line of CO_2 in the shock tube and the laser emission line. On the other hand, emission measurements done with CO_2 at 10.6 μm have shown that we can neglect the contribution of emission in that range of wavelengths.

The temperature and density obtained are average values since the laser beam crosses the shock tube section, and they are then integrated along a cylinder of 8.5 cm long and 2 mm in diameter because we suppose that the mixing has quickly reached its equilibrium temperature. The CO_2 absorption coefficient given by relation (27) is a function of the temperature and density of CO_2 within CO_2-Ar or CO_2-He mixing zones. Thus, for each line we can write

$$\alpha=\alpha_\omega(T,\rho) . \tag{29}$$

So if we accurately know the CO_2 absorption coefficient $\alpha_\omega(T,\rho)$ in the CO_2-Ar or CO_2-He mixing zones for two given lines, we can access to the values of T and ρ within these zones by solving the system of two equations:

$$\begin{aligned} \alpha_1&=\alpha_{\omega_1}(T,\rho) , \\ \alpha_2&=\alpha_{\omega_2}(T,\rho) , \end{aligned} \tag{30}$$

where ω_1 and ω_2 are the frequencies of the first and the second lines, respectively. The accuracy of the method depends on both the choice of the couple of gases which constitute the mixing and the absorption line. For the purpose of the present study, a selection was made of the best couple of frequency bands, as to the signal-to-noise ratio.

Absorption by the test gas CO_2 in the mixing zone of two continuous CO_2 laser lines, corresponding to transition between the vibrational levels $00°1 \rightarrow 10°0$ (about 10.4 μm wavelength), yields average profiles of density, temperature, and CO_2 mass concentration in the mixing zone. Error bars have been estimated to be $\pm 8\%$ near pure CO_2 and a little larger, because of the decrease of CO_2, but less than $\pm 12\%$, near pure argon or helium.

V. RESULTS AND DISCUSSION

As was said before, when the shock wave interacts with the 1.5-μm thin membrane, a CO_2-Ar or CO_2-He mixing appears, because of the local vorticities and instabilities. Initially, the temperature distribution should be caused by heat diffusion in the mixing zone, but quickly, turbulence dominates, leading to a rapid temperature and concentration equilibrium.

First, if we compare the theoretical results calculated from the Rankine-Hugoniot equations to the experimental values obtained in pure gases (on both sides of the mixing region), we see that our experimental results are very close to the calculated values of temperature and density in pure gases: for the CO_2-Ar case we obtain $T(CO_2)=765$ K, $\rho(CO_2)=0.17$ kg/m^3, and $T(Ar)=1240$ K and for the CO_2/He case we obtain $T(CO_2)=637$ K, $\rho(CO_2)=0.08$ kg/m^3, and $T(He)=548$ K. Results showing the evolutions to temperature and density within the mixing region are presented in Figs. 3 and 4 for the CO_2-Ar and Figs. 5 and 6 for CO_2-He. The most important result that is observed is that the evolution of temperature in the CO_2-Ar mixing zone seems to be more regular than in the case of the CO_2-He mixing region. One can say that the CO_2 and the argon diffuse into each other slowly and more regularly. In the CO_2-He case, the system progresses in a more rapid way, and the mixing does not occur in a uniform way. The temperature profile is affected and the mixing seems to be largely composed of helium because its temperature quickly reaches that of this pure gas. Here, we make clear the importance and influence of the Atwood number on the evolution of the mixing. The effect of the Atwood number is also visible when we compare the thicknesses of the two mixing zones: 36 mm for the CO_2-He case with $|A_t|_{CO_2\text{-He}} \approx 0.80$ and 26 mm for the CO_2-Ar case with $|A_t|_{CO_2\text{-Ar}} \approx 0.26$. During the interpenetration of the two gases, all perturbations present at the interface are amplified—the more so, the larger product $A_t * \Delta U$. The vorticity rise at the interface is advected in the mixing zone, and widens. Then, thermodynamic equilibrium establishes rapidly, due more to turbulence than to molecular diffusion. On the other hand, the shape of the curves (for argon a regular evolution and for helium a sharp decrease followed by a residual slope) might tell something

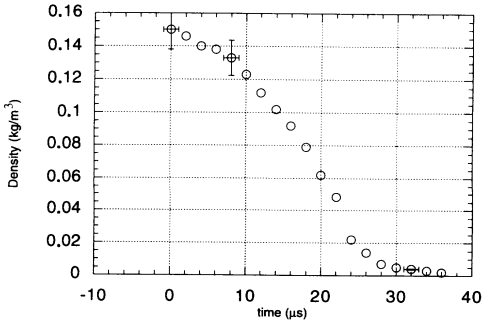

FIG. 3. Temperature profile within the CO_2-Ar incident mixing zone.

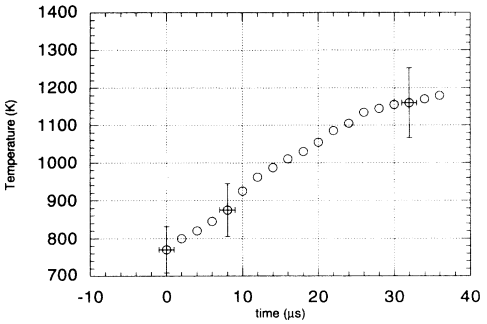

FIG. 4. Density profile within the CO_2-Ar incident mixing zone.

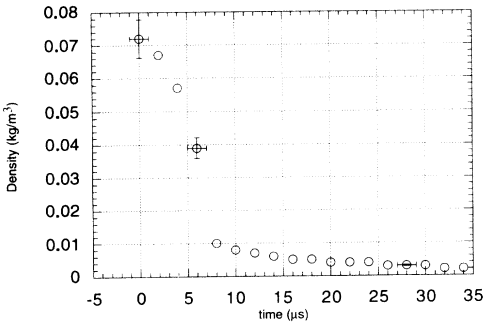

FIG. 5. Temperature profile within the CO_2-He incident mixing zone.

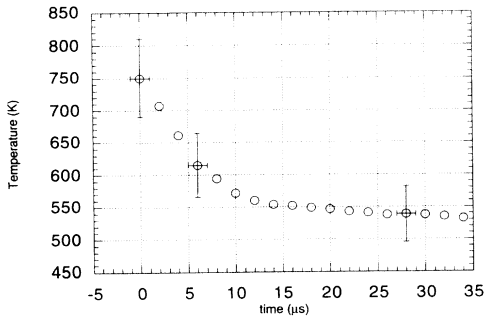

FIG. 6. Density profile within the CO_2-He incident mixing zone.

about the topology of the two mixing zones. One expects, as predicted by numerical studies [20], the penetration of CO_2 into helium to be in a form of long narrow jets because of the high Atwood number but that the interpenetration of CO_2 into argon is more regular. This leads us to think that the CO_2-He mixing zone should be composed of a greater percentage of helium downstream (in the pure helium side) and a strong concentration of CO_2 in the portion upstream. On the contrary, in the case of the CO_2-Ar mixing zone the interpenetration between the two gases occurs in a much more homogeneous way (low difference between the densities), and we obtain more regular profiles. Thus, one can say that the CO_2-Ar mixing zone is more homogeneous than the CO_2-He one.

VI. CONCLUSION

The infrared CO_2 laser absorption method, like many other optical or spectroscopical techniques, can contribute to the understanding of the shock induced Richtmyer-Meshkov mixing process in a shock tube, when one of the constituents of the mixing has appropriate spectroscopic properties. Even though the absorption measurements are averaged across the shock tube section, the fact that the only absorbent gas is CO_2 allows us to obtain some information on the dynamic and thermodynamic states of the shocked gaseous mixing zone. In the present study, our objective was not a diagnostic technique innovation, but to show that this preexisting method could be applicable, with some adaptation, to shock tube experiments, and could provide some helpful information about Richtmyer-Meshkov instability. Unfortunately, when the interaction of the shock and the mixing zone is too greatly influenced by three-dimensional boundary layer effects, then the signals obtained are hardly exploitable, and the method is no longer valid. From a dynamical point of view, we have emphasized the influence of the vorticity and the turbulent diffusion on the mixing process, as well as that of the Atwood number. We can say that, at the initial instants, the Atwood number plays an important role in the amplification of the instabilities, and, later, turbulent diffusion become predominant. Presently, our team is improving the absorption technique, using a multidirectional laser absorption method. This method could provide for several regions, instead of one, quantitative information about the wall boundary layer and three-dimensional effects which are quite significant in this kind of experiment.

ACKNOWLEDGMENTS

This work is supported by the C.E.A. Centre d'Etudes de Limeil-Valenton under Contract No. 1253/S 766 II Y. The authors want to thank Professor Jean Pourcin for many helpful discussions.

[1] Lord Rayleigh, Proc. London Math. Soc. **14**, 170 (1883).
[2] G. I. Taylor, Proc. R. Soc. London Ser. A **201**, 192 (1950).
[3] R. D. Richtmyer, Commun. Pure Appl. Math. **13**, 297 (1960).
[4] Y. Y. Meshkov, NASA Report No. TT F-13, 074, 1970 (unpublished).
[5] K. O. Mikaelian, Phys. Fluids **2**, 592 (1990).
[6] J. Y. Wang, Appl. Opt. **15**, 768 (1976).
[7] R. K. Hanson and P. K. Falcone, Appl. Opt. **17**, 2477 (1978).
[8] W. Cheng and F. Bien, AIAA J. **19**, 1071 (1981).
[9] E. C. Rea, Jr. and R. K. Hanson, Appl. Opt. **15**, 768 (1986).
[10] L. Houas, A. Farhat, and R. Brun, Phys. Fluids **31**, 807 (1988).
[11] L. Houas, A. Farhat, A. Ramdani, J. Fortes, and R. Brun, *Concentration and Temperature Profiles in a Shocked Gaseous Interface,* Proceedings of the 16th International Symposium on Shock Waves and Shock Tubes, edited by H. Grönig (VCH Physik Verlag, Aachen, 1987), p. 831.
[12] R. L. Abrams, Appl. Phys. Lett. **25**, 609 (1974).
[13] W. H. Christiansen, G. J. Mullaney, and A. Hertzberg, Appl. Phys. Lett. **18**, 385 (1971).
[14] C. Freed and A. Javan, Appl. Phys. Lett. **17**, 53 (1970).
[15] S. A. Munjee and W. H. Christiansen, Appl. Opt. **12**, 993 (1973).
[16] G. Hertzberg, *Molecular Spectra and Molecular Structure* (Van Nostrand, Princeton, 1945), Vol. II.
[17] S. S. Penner, *Quantitative Molecular Spectroscopy and Gas Emissivities* (Addison-Wesley, Reading, MA, 1959).
[18] O. V. Achasov, N. N. Kundriatsev, S. S. Novikov, R. I. Solukhin, and N. A. Fomin, *Diagnostica Neravnovesneir v Moleculiarneir Laserar* (Nauka I Ternika, Minsk, 1985).
[19] O. V. Achasov, N. A. Fomin, S. A. Labuda, D. S. Ragozin, and R. I. Solukhin, Rev. Phys. Appl. **17**, 15 (1982).
[20] D. L. Youngs, Physica D **12**, 32 (1984).

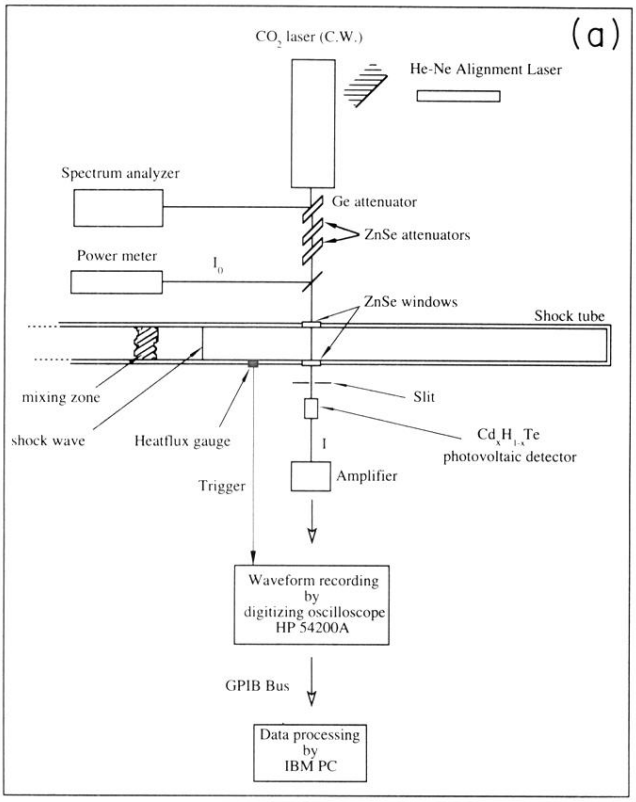

Absorption signal of CO_2 -Ar mixing;Mach number 4

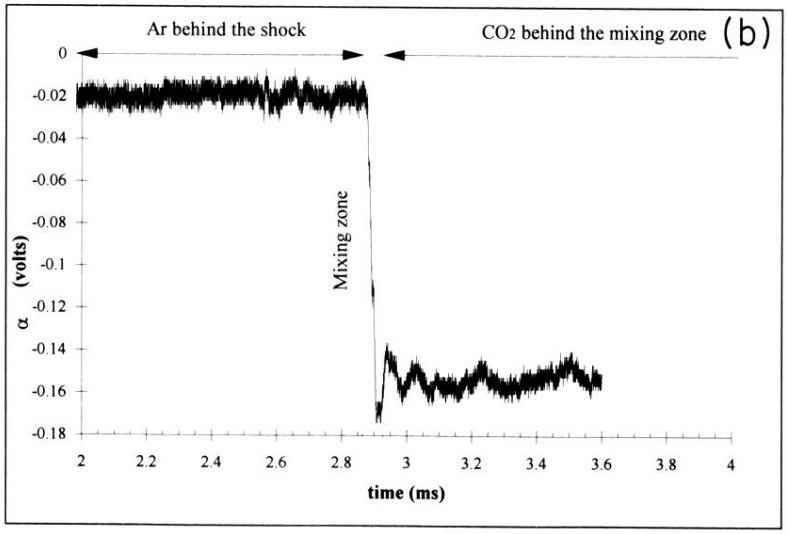

FIG. 1. (a) Sketch of the experimental set-up; (b) typical absorption signal record.